

PROCESS DEVELOPMENT ON PHOTOLITHOGRAPHY FREE IBC SOLAR CELLS

Sukhvinder Singh¹, Barry O'Sullivan¹, Maria Recaman Payo¹, Angel Uruena De Castro¹,
Maarten Debucquoy¹, Jozef Szlufcik¹, Jef Poortmans^{1,2,3}

1. imec, Kapeldreef 75, B-3001 Leuven, Belgium, 2. KU Leuven, B-3001 Leuven Belgium, 3. U Hasselt, B-3590,
Diepenbeek, Belgium

Corresponding author: e-mail: Sukhvinder.Singh@imec.be, phone: +32-1628-1590

ABSTRACT: IBC process development at imec started with a small cell area baseline process on high quality FZ wafers. This resulted in cell efficiencies up to 23.3% for 4 cm² cells on 4-inch n-type FZ substrates. Later 12.5x12.5 cm² and 15.6 x 15.6 cm² semi-sq commercially available n-type CZ silicon wafers were successfully integrated in this baseline. Confirmed efficiencies up to 23.1 % on 4 cm² cells on 15.6 x 15.6 cm² wafer have been achieved. This baseline process involves three photolithography steps, extensive surface cleaning and various high temperature process steps. Based on this stable high-efficiency platform, steps to simplify this process and implementation of industrially viable novel processes were initiated. Initial steps towards process simplification have already been presented, concluding that reduced complexity of the process did not come at a cost of cell efficiency. In this study we show further simplification of the IBC cell process by demonstrating potential replacement of all photolithography steps by cost effective and industrially feasible process steps, namely laser ablation and screen printing. Best cell efficiency of 22.7 % has been achieved on newly developed photolitho-free IBC process. Furthermore the stability of baseline process is improved by implementing the adapted process recipe for back surface field (BSF) diffusion.

Keywords: Back Contact, Back-Surface-Field, c-Si, Laser Processing, n-type, Screen Printing

1 INTRODUCTION

Interdigitated back silicon contact solar (IBC) cells can result in highly efficient solar cells. This is thanks to several advantages, including absence of front grid shading and lower series resistance due to the large metallized area. Record efficiencies up to 24.2 % have been demonstrated on IBC solar cells by SunPower on large area (155 cm²) CZ silicon substrates in production [1]. Other research institutes and companies have also demonstrated high efficiencies above 21 % on large area IBC cells on CZ silicon wafers in recent years. These include 22.4 % efficiency by Samsung/Varian on 155 cm² [2], 21.3 % by ISC Konstanz/Silfab on 243 cm² [3] and 22.1 % by ISFH/Bosch on approx. 240 cm² CZ wafers [4]. However these processes have not been implemented in production yet. The reasons possibly being either the large number of high cost and non-industrial process steps [2, 4] or limited efficiency gains with extra process steps [3].

In order to achieve an industrial large area high efficiency IBC solar cell process a platform based approach has been undertaken at imec. The goal of this platform is to first have a stable high efficiency baseline process on small area cells. The next step is aimed at implementing industrially viable process steps before finally scaling to large area wafers.

Following this approach, firstly a small area (4 cm²) baseline process for IBC silicon solar cells on high quality FZ wafers was developed at imec [5], resulting in efficiencies up to 23.3%. Subsequently 12.5x12.5 cm² [6] and 15.6 x 15.6 cm² n-type CZ silicon wafers were utilised, resulting in stable high efficiency platform, with values up to 23.1 % on small area (4 cm²) cells on 15.6 x 15.6 cm² CZ wafers. As presented previously [7], this baseline process involves three photolithography steps, extensive surface cleaning and various high temperature process steps. Thus next steps to implement industrially viable processes are initiated. Initial work on this topic has been reported previously [7,8]. In that work, it was

already demonstrated that the contact opening could be achieved with laser ablation instead of photolithography.

In this study we report on our efforts to further simplify the IBC cell process, by demonstrating potential replacement of the remaining two photolithography steps by cost effective and faster process steps, namely laser ablation and screen printing. Besides that we also improve stability of the baseline process by implementing an adapted recipe for back surface field (BSF) diffusion.

2 PROCESS FLOW

The baseline IBC flow at imec is summarised underneath. The changes in the process flow, developed in this work to simplify the flow, are also mentioned. Firstly, 15.6 x 15.6 cm² semi square n-type CZ silicon wafers undergo a saw damage removal etch step, are cleaned and undergo a diffusion with BBr₃. The emitter dopant drive-in and passivation is carried out by a wet thermal oxidation process. Then the back surface field regions are defined by patterning the oxide of the emitter by photolithography or by laser ablation (in section 2.2) followed by etching the boron doped layer from the opened areas. This is followed by a BSF diffusion (described in section 2.1), and a drive-in/passivation. Next, the front oxide is etched for enabling surface texturing. A cleaning is performed followed by front surface field diffusion, drive-in and ARC deposition. Contact areas are defined on both doped regions by laser ablation or photolithography. Metallization is carried out by PVD aluminium (Al-Si 1%) blanket deposition. Emitter and BSF metallised regions are defined by photolithography or by screen printing a resist followed by metal etching (Section 2.3). Finally the wafers are sintered and diced into solar cells (with an area of 2x2 cm²). The process developments of the above mentioned steps and obtained cell results are listed in the sections below.

2.1 Back surface field (BSF) diffusion.

As mentioned above the interdigitated doping for IBC cells are realized by locally removing the boron emitter and subsequent phosphorus diffusion and drive-in to form n-type BSF with target sheet resistance of 50 ohm/sq. Over the course of several iterations of IBC process at imec, significant variation in the BSF contact resistance was observed with values ranging from 0.3 m Ω .cm² to 1.5 m Ω .cm². This resistance greatly affects the series resistance and hence the fill factor (FF) of the cells. It may be noted that the BSF used in the present case is moderately doped and non-selective, unlike highly doped and selective BSF under the contacts as used elsewhere [9]. The BSF recipe in the present case is balanced between limiting recombination losses and contact resistance losses. It has been reported that the specific contact resistance (ρ_c) for aluminium on n-type Si is very sensitive to the surface concentration of the doping (N_d) [10]. ρ_c could change from 10⁻³ to <10⁻⁴ Ω .cm² for a change in surface concentration of 10¹⁹/cm³ to 2 x 10¹⁹/cm³. In order to avoid the limitation of the fill factor by contact resistance of BSF region, process parameters for BSF doping were adapted to achieve slightly higher surface concentration, as shown in the SIMS profiles for the baseline and adapted BSF processes, displayed in Fig 1. Using the adapted recipe $\rho_{\text{contact,BSF}}$ decreased from 1.5 m Ω .cm² to 0.5 m Ω .cm², whereas $J_{0,\text{BSF}}$ increased from 44 to 55 fA/cm².

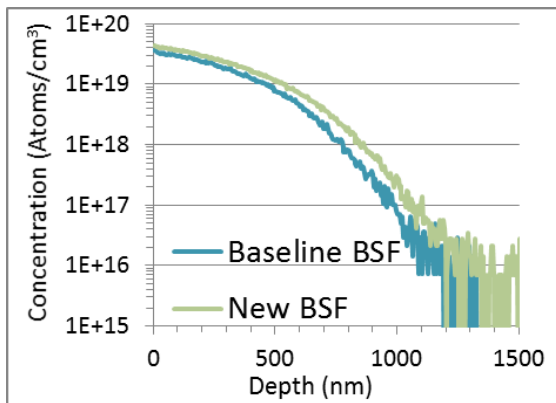


Figure 1: SIMS profiles for the two BSF diffusions described in this work.

Table I: The average cell data for IBC cells processed with the baseline and adapted BSF

	J_{sc} [mA/ cm ²]	V_{oc} [mV]	FF [%]	η [%]	$J_{0,\text{BSF}}$ [fA /cm ²]	$\rho_{\text{contact,BSF}}$ [m Ω .c m ²]
Base line	41.20 ± 0.1	691 ± 2	75.9 ± 3.5	21.6 ± 1.0	44	1.5
Ad. BSF	41.36 ± 0.2	691 ± 1	78.8 ± 1.4	22.7 ± 0.4	55	0.5

The average IBC cell data for cells processed with the baseline and modified BSF POCl₃ diffusion process is presented in Table I, where it is clear that the adapted BSF profile results in a large FF increase, compared to the baseline process.

2.2 Laser ablation for BSF definition

As reported above, laser ablation for contact opening has been successfully implemented at imec [7]. Now we investigate the feasibility of this technique for opening emitter prior to BSF diffusion. As this is the first patterning step in the IBC process flow, alignment marks are also defined at this step to enable successive patterns to overlap. Process parameters such as laser speed, line overlap and power were investigated and optimized for uniform opening (Fig 2). Example figures showing the case of (a) excessive laser speed/insufficient line overlap between lines or (b) excessive overlap within one line (c) insufficient laser power/line overlap, thereby resulting in non-ablated regions within the region to be ablated. Optimum conditions shown in Fig 2 (d) are chosen, thereby ensuring sufficient overlap to result in stable cross-wafer ablation. Furthermore selective etching of the underlying emitter in the ablated areas was also optimised to remove laser damage, prior to the BSF diffusion process. The efficiency of the etch to remove laser induced damage was verified by comparing the J_0 values on ablated and non-ablated regions after the subsequent BSF diffusion, where similar values were measured.

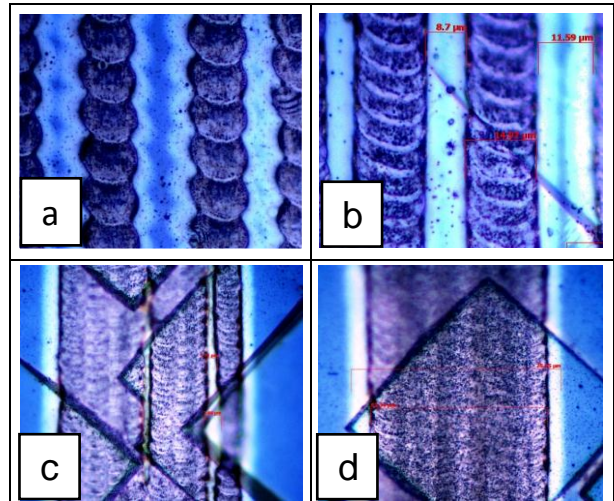


Figure 2: Optical microscopy images of laser ablated oxidised silicon wafers at different processing conditions.

2.3 Screen printing for metal patterning

IBC metallization is carried out by blanket deposition of aluminium (Al-Si) by PVD. In our previous work, the emitter and BSF metallised areas were defined by a photolithography step and separated by etching back the metal. In the present work a polymer is screen printed to replace the photo-lithography step. In this case, the polymer resist is printed, after blanket Al-Si layer deposition (depicted by black area in Fig 3 (a)). The Al-Si layer is chemically etched followed by removal of the polymer paste.

Various critical tests were carried out before implementing screen printing step in the IBC baseline flow. Tolerance of the printed resist to the chemicals used for etching the metal layer was confirmed. Because screen printing pattern resolution is limited by the screen (mesh and emulsion), sufficient print width and margins are required to limit risk of interruption or shunting of

two closely printed resist lines.

Compatibility with the screen printer was verified by assessing the cross-wafer print-induced pattern shift, average stretching of screen along x-axis and y-axis (squeegee print direction). From these tests the measured stretching of screens is found to be between 30 and 70 μm over the length of silicon wafer (15.6 cm), depending on the type of screen (mesh) used. Error in alignment capability of screen printer is $\pm 15 \mu\text{m}$.

After taking into account the screen stretch, the alignment capability of the tool and the print width/margins needed to avoid shunting, a screen was designed. The 25 cells on this pattern incorporate variations in spacing between BSF metal and emitter metal (represented as X in Fig 3 (a)). It should be noted this spacing is significantly larger than what is possible with photolithography. Clearly, this limits the width of the metal on the BSF finger ($W_{\text{metal,BSF}}$).

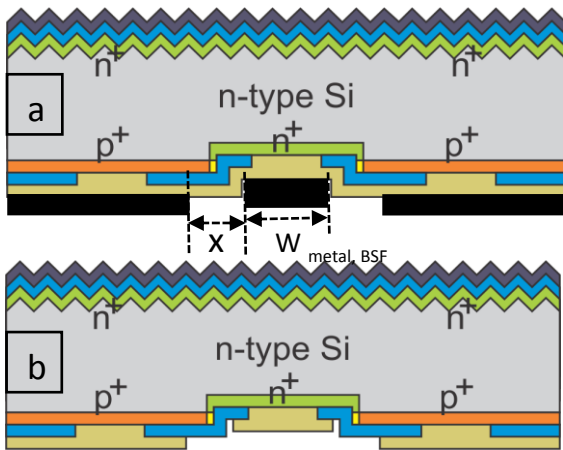


Figure 3: Schematic of IBC cell

Table II. Comparison of best cell efficiencies of photolitho baseline and photolitho-free cell processes

	J_{sc} [mA/c m^2]	V_{oc} [mV]	FF [%]	η [%]
Photolitho baseline	41.21	690	79.5	22.6
Photo-litho-free	41.50	688	79.5	22.7

The effect of $W_{\text{metal,BSF}}$ on the IV characteristics is studied. Short circuit current and open circuit voltage are not affected by $W_{\text{metal,BSF}}$ (not shown), within the range tested. However the average fill factor (FF) of cells increases with $W_{\text{metal,BSF}}$ as shown in Fig 4. Fig 4 also shows the FF for best case (by photolithography) and the calculated curve by including effect of line resistance due to limited metal width. The calculated curve fits well with the measured average values for screen printed case.

The cell efficiencies for best case photolitho based and photolitho-free cases are listed in Table II. As seen from the table the best cells parameters and efficiencies are similar for both cases.

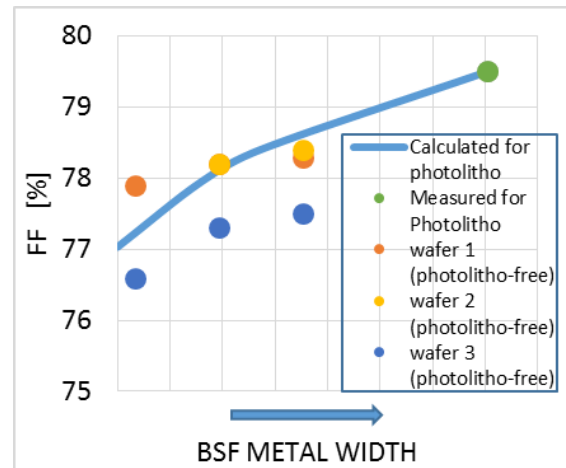


Figure 4: Effect of BSF metal width on FF of IBC cells.

The key finding in this paper is the ability to pattern IBC wafers with industrially viable processing techniques, and maintain high cell efficiency. This is a first step towards large area high efficiency IBC solar cells, but clearly demonstrates a proof of concept for such a process flow.

3 CONCLUSIONS

Recent developments on an IBC platform have been presented. Results include a modification of the BSF diffusion profile, reducing contacting resistance, and consequently increasing FF and efficiency. A proof of concept process flow for industrially viable IBC solar cell processing has also been developed. In this flow, patterning has been performed by laser patterning and screen printing. Best efficiency of 22.7 % has been achieved on small area IBC solar cells with this photolitho-free process.

5 ACKNOWLEDGEMENTS

The authors gratefully acknowledge the financial support of imec's industrial affiliation program and of the European Union's Seventh Programme for research, technological development and demonstration under grant agreement No 308350. The authors would also like to thank Sun Chemical for providing screen printable resist inks.

6 REFERENCES

- [1] PJ Cousins et. al., 35th IEEE Photovoltaic Specialists Conference (2010) 275.
- [2] C.B. Mo et al., 27th EUPVSEC, Frankfurt, Germany (2012).
- [3] A. Halm et al., 27th EUPVSEC, Frankfurt, Germany (2012).
- [4] Bosch SE, press release (2013).
- [5] M Aleman et. al. 2nd SiliconPV, Leuven (2012).
- [6] N E Posthuma et. al, 27th EUPVSEC, Frankfurt Germany (2012).
- [7] BJ O'Sullivan et. al. 28th EUPVSEC, Paris, France (2013).
- [8] S. Singh et. al. 28th EUPVSEC, Paris, France (2013).

-
- [9] K. C. Fong et. al. 28th EUPVSEC, Paris, France (2013).
[10] S. Swirhun, Electrochem. Soc. Oct. (1988).